INVITED PAPER *Special Section on Recent Advances in Simulation Techniques and Their Applications for Electronics*

Optical Waveguide Theory by the Finite Element Method

Masanori KOSHIBA[†a)], ***Fellow***

SUMMARY Recent progress in research on the finite element method (FEM) for optical waveguide design and analysis is reviewed, focusing on the author's works. After briefly reviewing fundamentals of FEM such as a theoretical framework, a conventional nodal element, a newly developed edge element to eliminate nonphysical, spurious solutions, and a perfectly matched layer to avoid undesirable reflections from computational window edges, various FEM techniques for a guided-mode analysis, a beam propagation analysis, and a waveguide discontinuity analysis are described. Some design examples are introduced, including current research activities on multi-core fibers.

key words: *finite element method, beam propagation method, spurious solutions, fiber optics, nanophotonics*

1. Introduction

Recent advances in the field of guided-wave optics, such as fiber optics and nanophotonics, have included the introduction of arbitrarily-shaped optical waveguides which, in many cases, also happened to be inhomogeneous, dissipative, anisotropic, and/or nonlinear. Most of such cases of waveguide arbitrariness do not lend themselves to analytical solutions and therefore, computational tools for modeling and simulation are essential for successful design, optimization, and realization of high-performance optical waveguides. For this purpose, various numerical techniques have been developed. In particular, the finite element method (FEM) is a powerful and efficient tool for the most general guided-wave problems. Its use in both the research community and the commercial sector is extensive, and indeed it could be said that without it many optical waveguide problems would be incapable of solution.

Over the last few decades, the author and his coworkers have developed new numerical formulations and techniques based on FEM for design and analysis of optical fibers and nanophotonic devices/circuits that have contributed to the advancement of computational photonics. In this paper, recent progress in FEM research is reviewed, focusing on the author's works. After briefly reviewing fundamentals of FEM such as a theoretical framework, a conventional nodal element, a newly developed edge element to eliminate nonphysical, spurious solutions, and a perfectly matched layer (PML) to avoid undesirable reflections from computational window edges, various FEM techniques for a guided-mode analysis, a beam propagation analysis, and a waveguide discontinuity analysis are described. Some design examples are introduced, including current research activities on multi-core fibers (MCFs).

Manuscript received September 19, 2013.

[†]The author is with Hokkaido University Career Center, Sapporo-shi, 060-0808 Japan.

a) E-mail: koshiba@ist.hokudai.ac.jp

DOI: 10.1587/transele.E97.C.625

2. Fundamentals of Finite Element Method

2.1 Theoretical Framework

In FEM, instead of differential equations for the system under consideration, corresponding functionals (variational expressions) to which a variational principle is applied are set up, where the region of interest is divided into the so-called elements as shown in Fig. 1. In FEM, an equivalent discretized model for each element is considered and then, all the element contributions to the system are assembled. In other words, FEM can be considered a subclass of the Ritz method, in which piecewise defined polynomial functions are used for trial functions and infinite degrees of freedom of the system are discretized or replaced by a finite number of unknown parameters.

Elements can have various shapes, allowing the use of a non-uniform mesh. Therefore, FEM is suitable for problems with very steep variations of fields. Furthermore, this approach can be easily adopted into inhomogeneous and anisotropic problems, and it is possible to systematically increase the accuracy of solutions obtained, as necessary. In addition, FEM can be established not only by the variational method but also by the Galerkin method which is a weighted residual method. Therefore, FEM may be applicable to lossy and/or leaky optical waveguides, where a variational principle does not exist or cannot be identified.

2.2 Nodal and Edge Elements

Various elements are available in FEM. Figures 2 and 3 show conventional nodal elements. Triangular and tetrahedral elements are utilized for two-dimensional and three-

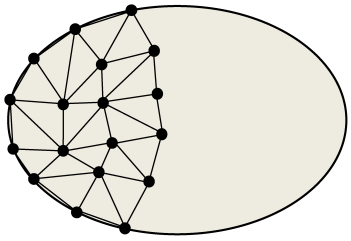

Fig. 1 Element division.

dimensional problems, respectively. The lowest-order or linear element employs the first-order polynomial. The quadratic element, on the other hand, employs the second-order polynomial.

The most serious difficulty in applying FEM to electromagnetic wave problems was the appearance of nonphysical, spurious solutions. Consequently, the development of a method to suppress or eliminate such spurious solutions was pressingly needed.

The spurious solutions can be characterized as

$$\nabla \times \boldsymbol{\Phi} = \mathbf{0} \tag{1}$$

with $\boldsymbol{\Phi}$ being the electric field $\boldsymbol{E}$ or the magnetic field $\boldsymbol{H}$. Considering that the electromagnetic fields have to be tangentially continuous across material interfaces and eliminating some of null-space degrees of freedom corresponding to irrotational, spurious fields expressed as Eq. (1) from trial fields, the so-called edge elements as shown in Figs. 4 and 5 have been developed [1], [2].

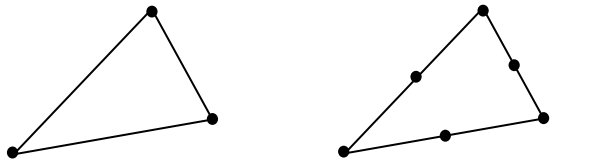

(a) Linear element. (b) Quadratic element.

Fig. 2 Triangular nodal elements.

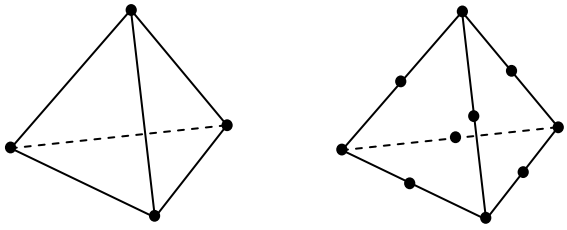

(a) Linear element. (b) Quadratic element.

Fig. 3 Tetrahedral nodal elements.

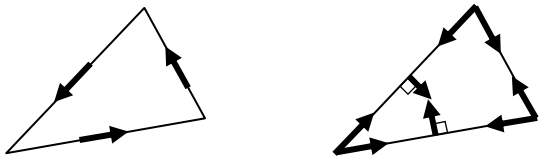

(a) Constant tangential and linear normal (CT/LN) element. (b) Linear tangential and quadratic normal (LT/QN) element.

Fig. 4 Triangular edge elements.

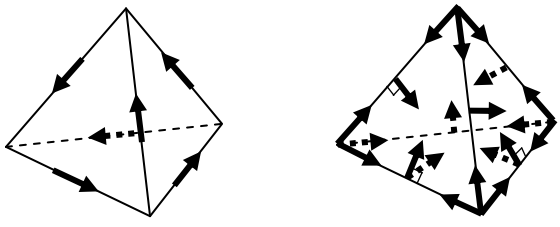

(a) Constant tangential and linear normal (CT/LN) element. (b) Linear tangential and quadratic normal (LT/QN) element.

Fig. 5 Tetrahedral edge elements.

The lowest-order triangular and tetrahedral edge elements, which employ three and six variables, respectively, are based on constant tangential and linear normal (CT/LN) vector basis functions. The tangential component of a particular CT/LN basis function is constant along one edge of triangle and tetrahedron, and is zero along the other edges, while the normal component is a linear function along all edges. The higher-order triangular and tetrahedral edge elements, which employ eight and twenty variables, respectively, are based on linear tangential and quadratic normal (LT/QN) vector basis functions.

2.3 Perfectly Matched Layer

When simulating optical waveguide devices and/or circuits, in order to reduce spurious reflections from the computational window edges, the use of appropriate absorbing boundary conditions is indispensable. For this purpose, the PML condition [3] was developed. Unfortunately, since the earlier PML technique involves a modification of Maxwell's equations based on the splitting of field components into two subcomponents, these non-Maxwellian equations do not have a desirable form for the FEM formulations. Recently, the so-called anisotropic PML, which does not involve the field splitting, was developed [4] and has been widely used for mesh truncation in the FEM analysis.

We consider a three-dimensional domain surrounded by PML regions 1 to 7 with thickness $d_i\,(i=1, 2, 3)$ as shown in Fig. 6. A non-PML region has dimensions a, b, and c in the x, y, and z directions, respectively. Using the anisotropic PML, the PML permittivity and permeability tensors are written as

$$[\varepsilon]_{\mathrm{PML}} = s_x s_y s_z [S][\varepsilon][S] \tag{2a}$$

$$[\mu]_{\mathrm{PML}} = s_x s_y s_z [S][\mu][S] \tag{2b}$$

with

$$[S] = \begin{bmatrix} 1/s_x & 0 & 0 \\ 0 & 1/s_y & 0 \\ 0 & 0 & 1/s_z \end{bmatrix} \tag{3}$$

where $[\varepsilon]$ and $[\mu]$ are, respectively, the permittivity and permeability tensors of the original PML regions. PML parameters s_x, s_y, s_z are listed in Table 1, where the values of s_i in Table 1 are real for bounded-field problems as

$$s_i = 1 + \alpha_i \tag{4}$$

and they are complex for unbounded-field problems as

$$s_i = 1 - j\alpha_i \tag{5}$$

Attenuation of the electromagnetic field in PML regions can be controlled by choosing appropriate values of α_i and we

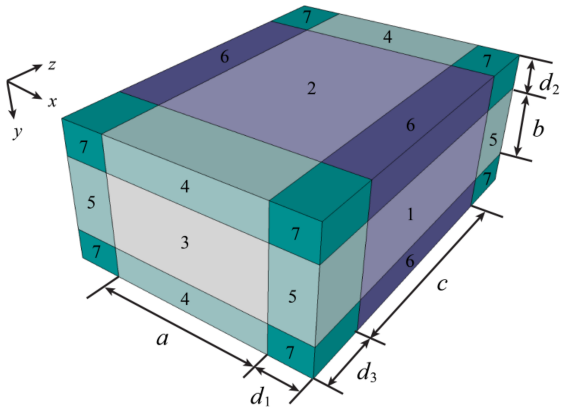

Fig. 6 Computational domain surrounded by perfectly matched layers.

Table 1 Perfectrly matched layer (PML) parameters.

PML parameter	PML region						
	1	2	3	4	5	6	7
s_x	s_1	1	1	1	s_1	s_1	s_1
s_y	1	s_2	1	s_2	1	s_2	s_2
s_z	1	1	s_3	s_3	s_3	1	s_3

For two-dimensional problems, which are uniform in the x, y, and z directions, s_x, s_y, and s_z are set to 1, respectively.

assume parabolic profiles of α_i as

$$\alpha_i = \alpha_{i,\mathrm{MAX}} (\rho/d_i)^2 \tag{6}$$

where ρ is the distance from the beginning of PML and the subscript "max" denotes the maximum value.

3. Guided-mode Analysis

3.1 Straight Waveguide Analysis

Although a formulation based on a single scalar quantity is inadequate for the general guided-mode analysis, the useful approximation can be found for weakly guiding structures and the so-called approximate scalar FEM has been developed [5], [6]. In the approximate scalar FEM, conventional nodal elements can be used and spurious solutions do not occur. However, to rigorously evaluate guided-modes in strongly guiding structures such as high-index contrast (HIC) waveguides, photonic crystal (PC or PhC) waveguides, hole-assisted fibers (HAFs), and photonic crystal fibers (PCFs) which are grouped into holey fibers (HFs) with index-guiding effect and photonic band-gap fibers (PBGFs) with photonic band-gap effect, a full vector analysis is necessary, and different types of full vector FEM have been developed. Here, the electromagnetic field with a time (t) dependence of the form $\exp(j\omega t)$ is expressed as

$$\boldsymbol{\Phi} = \boldsymbol{\phi}(x, y) \exp[j(\omega t - \beta z)] \tag{7}$$

where z is the propagation direction, ω is the angular frequency, and β is the propagation constant.

Of the various formulations, the FEM using full vector electric or magnetic field is quite suitable for a wide range of practical, complicated problems. The most serious problem associated with this approach is the appearance of spurious solutions. The penalty function method (PFM) has been widely used to cure this problem [7]–[9], but in this technique, an arbitrary positive constant, called the penalty coefficient, is involved and the accuracy of solutions depends on its magnitude. Furthermore, in PMF, the propagation constant is first given as an input datum, and subsequently the operating angular frequency or the operating wavelength is obtained as a solution.

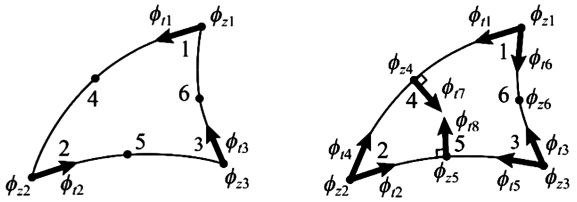

(a) CT/LN edge element and linear nodal element.

(b) LT/QN edge element and quadratic nodal element

Fig. 7 Curvilinear hybrid edge/nodal elements.

In order to overcome these issues in PFM, edge elements have been introduced into the guided-mode analysis of a waveguide with arbitrary cross section in the xy (transverse) plane [10]–[12], and curvilinear hybrid edge/nodal elements with triangular shape as shown in Fig. 7 were developed [12].

Figure 7(a) shows the lowest-order hybrid element which is composed of a CT/LN edge element with three variables for transverse fields and a linear nodal element with three variables for axial fields [10]. Figure 7(b) shows the higher-order hybrid element which is composed of a LN/QT edge element with eight variables and a quadratic nodal element with six axial variables. Removing ϕ_{t7} and ϕ_{t8} from the LT/QN element, we can obtain another higher-order hybrid element composed of a linear tangential and linear normal (LT/LN) element and a quadratic nodal element [11]. Curvilinear hybrid elements can give faster convergence than rectilinear hybrid elements and when using a curvilinear hybrid element composed of a LN/QT edge element and a quadratic nodal element, significantly fastest convergence is obtained, irrespective of values of the operating wavelength (input datum) [12].

3.2 Curved Waveguide Analysis

A curvilinear hybrid edge/nodal element has been used not only for a straight optical waveguide analysis but also for a curved optical waveguide analysis. In [13], a full vector FEM was formulated in a local cylindrical coordinate system and an anisotropic PML was implemented to the computational window edges.

Recently, using this approach, a bend-insensitive and effectively single-moded all-solid PBGF (AS-PBGF) with heterostructured cladding was designed and fabricated [14]. Figures 8(a), (b), and (c) show a typical AS-PBGF (uniform structure), a segmented cladding structure, and a wind-

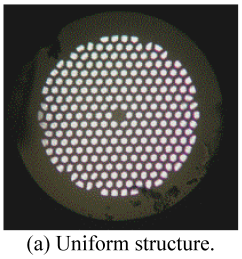

(a) Uniform structure.

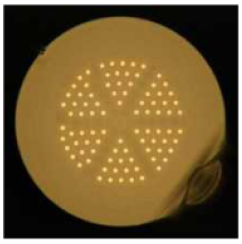

(b) Segmented cladding structure.

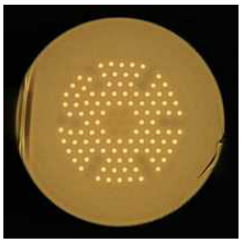

(c) Windmill structure.

Fig. 8 All-solid photonic band-gap fiber with heterostructured cladding [14].

mill structure, respectively. In Fig. 9, the bending losses as a function of bend radius at 1550-nm wavelength are presented for these structures. We can see that the bending loss of the windmill structure is effectively low and compatible to that of the multi-moded 7-cell-core uniform structure. Therefore, the windmill structure based on the heterostructured cladding exhibits both low bending losses and low confinement losses while keeping single-mode operation, which is one of the issues in a solid core PBGF.

4. Beam Propagation Analysis

4.1 Beam Propagation Method

The beam propagation method (BPM) is at present the most widely used for the study of light propagation in longitudinally varying waveguides. Under the slowly varying envelope approximation (SVEA), the electromagnetic field is expressed as

$$\boldsymbol{\Phi} = \boldsymbol{\phi}(x, y, z) \exp[j(\omega t - \beta_0 z)] \tag{8}$$

where $\boldsymbol{\phi}$ is the slowly varying complex amplitude and β_0 is the reference propagation constant which can be renewed at every propagation step.

In the BPM based on FEM (FE-BPM), the field in the transverse (xy) plane is discretized with FEM and the Crank-Nicholson algorithm is applied to the propagation

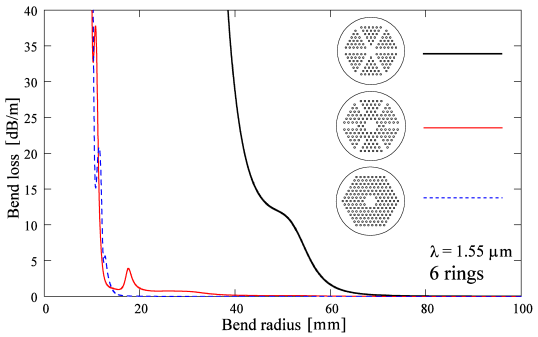

Fig. 9 Bending losses as a function of bend radius for 7-cell-core uniform, segmented cladding, and windmill structures [14].

(z) direction. It is possible to use non-uniform finite element meshes and these meshes can be adaptively updated along the propagation direction so that computational efficiency can be improved without degrading numerical accuracy. Simple and efficient mesh generation algorithms for an approximate scalar FE-BPM analysis [15] and a full vector FE-BPM analysis [16] have already been developed.

One of the key issues in implementing FE-BPM to study light propagation in a finite spatial domain is the boundary condition at the computational window edges. Recently, an anisotropic PML has been effectively implemented not only to a two-dimensional FE-BPM (2D-FE-BPM) [17] for planar optical waveguides but also to an approximate scalar three-dimensional FE-BPM (3D-FE-BPM) [18] and a full vector 3D-FE-BPM [19] for arbitrarily-shaped optical waveguides.

Recently, using the approximate scalar 3D-FE-BPM, a low-loss and broadband mode (de)multiplexer based on a directional coupler (DC) and a wavelength insensitive coupler (WINC) as shown in Fig. 10 was designed and fabricated for mode-division multiplexing (MDM) transmission [20], where a silica-based planar lightwave circuit (PLC) is used. Figures 11(a) and (b) show, respectively, the numerical and the experimental results of the wavelength dependence of the transmission of the mode (de)multiplexer at port 4 when the LP_{01} mode is input into port 1 or port 2. The inset images in Fig. 11(b) show near field patterns measured at wavelengths of 1060 nm, 1310 nm, and 1550 nm. Excepting the radiation loss due to the mode field diameter mismatch between the input/output fiber and the PLC waveguide, the experimental results agree well with the numerical results and it is confirmed that the broadband mode conversion from the LP_{01} mode to the LP_{11} mode is realized by using the WINC-based mode multiplexer.

4.2 Imaginary Distance Beam Propagation Method

It should be noted that the so-called imaginary distance BPM (ID-BPM) has been reported as an analysis method of guided modes. In ID-BPM, the propagation direction is selected along the imaginary axis and selecting the appropriate propagation step size, we can extract the specific guided mode from the initial input field. There are a number of

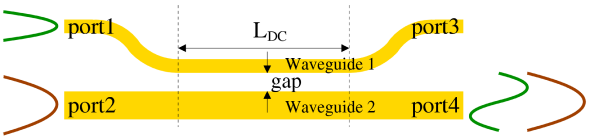

(a) Mode (de)multiplexer based on directional coupler (top view).

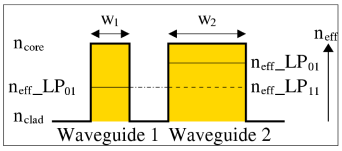

(b) Effective index for mode conversion (cross-sectional view).

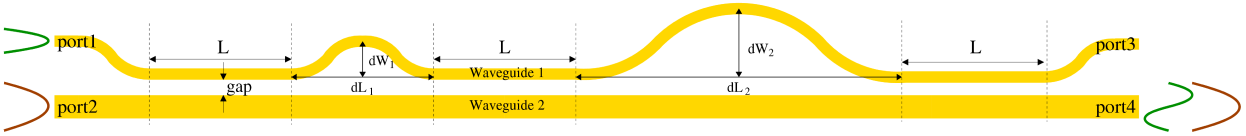

(c) Mode (de)multiplexer based on wavelength insensitive coupler (top view).

Fig. 10 Structures of mode (de)multiplexers [20].

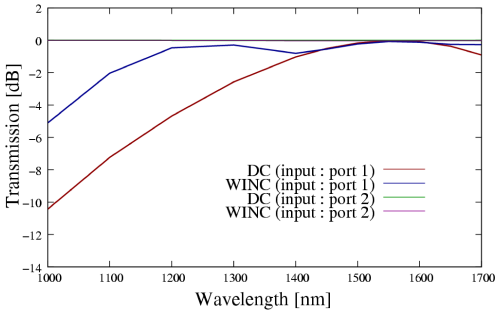

(a) Theoretical results.

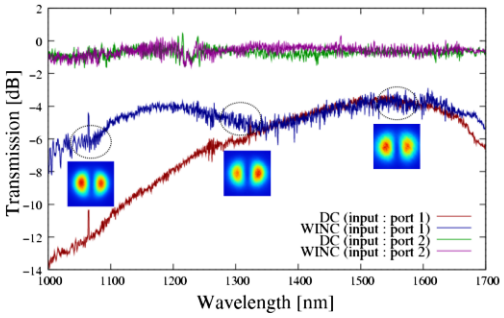

(b) Experimental results.

Fig. 11 Wavelength dependence of the transmission of mode (de) multiplexers at port 4 [20].

versions of ID-BPM. In the ID-BPM based on FEM (FE-ID-BPM), to evaluate propagation losses of leaky modes, an anisotropic PML is employed as a boundary condition at computational window edges. Both an approximate scalar FE-ID-BPM [21] with conventional nodal elements and a full vector FE-ID-BPM [22] with hybrid edge/nodal elements have already been developed.

In particular, the full vector FE-ID-BPM has been effectively applied to characterizing various PCFs such as HFs [23],[24] and PBGFs [25]. To model PCFs accurately, especially with large air holes or high-index rods, it is crucial to use a full vector model. FEM is useful not only for idealized-model simulations but also for realistic-model simulations based on actual fiber structures [26]. A curvilinear hybrid element composed of a LN/QT edge element and a quadratic nodal element shown in Fig. 7(b) is useful for accurately modeling the curved boundaries of air holes and high-index rods.

Here, we consider a fabricated dispersion compensating PCF (DCPCF) [27] as shown in Fig. 12(a), which is based on a concentric dual core refractive index profile, where the ring core (second air-hole ring from the central core) is formed by reducing the air-hole size. The diameter of outer cladding air-holes is tailored to control the dispersion slope as well as the confinement loss. The air-holes surrounding the inner core are not circular in shape and two opposing holes are smaller than the other four. This makes this fiber highly birefringent and the two fundamental core modes become polarization-split. One mode will be polarized along the slow-axis and the other along the fast-axis. Figure 12(b) shows the finite element mesh used in the full vector FE-ID-BPM simulation [28], where the number of hybrid edge/nodal elements is 47,000 and the number of the unknowns is 327,000. Anisotropic PML boundaries are applied to enable the calculation of the precise leakage loss of the fiber. Figure 12(c) shows the electric field distribution of the slow-axis mode at 1550-nm wavelength [28]. The mode is well confined to the inner core. The effective area of the realistic fiber was calculated to be 1.81 μm^2 at 1550 nm, which is slightly smaller than the value of effective area of 2.0 μm^2 of the fabricated DCPCF [27].

Recently, using the full vector FE-ID-BPM, a bending-insensitive single-mode HAF with two air-hole rings was designed and fabricated [29] as shown in Fig. 13. A circular bend structure was replaced by a straight fiber with equivalent refractive index and an anisotropic PML was used along the radiation direction. Figure 14 shows the theoretical and experimental bending loss of HAF with two air-hole rings as a function of bending radius at 1550-nm wavelength. We can see that the bending loss of the HAF is much less than that of the standard single-mode fiber (SMF), especially for small bending radius. The theoretical results are in good agreement with the experimental results.

5. Waveguide Discontinuity Analysis

5.1 Frequency-domain Analysis

BPM assumes only the forward propagating waves and therefore, it is difficult to take into account backward reflec-

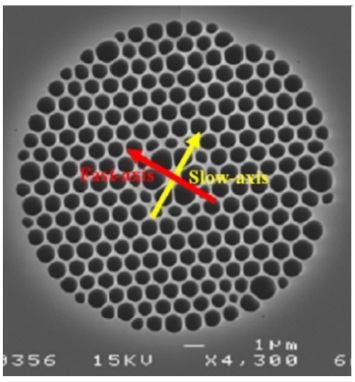

(a) Fabricated dispersion compensating photonic crystal fiber [27].

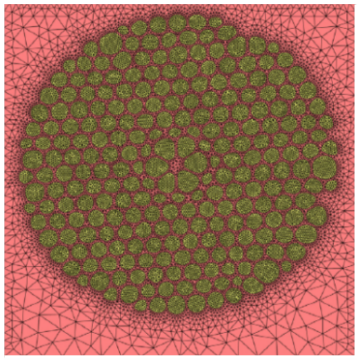

(b) Mesh with curvilinear hybrid edge/nodal elements [28].

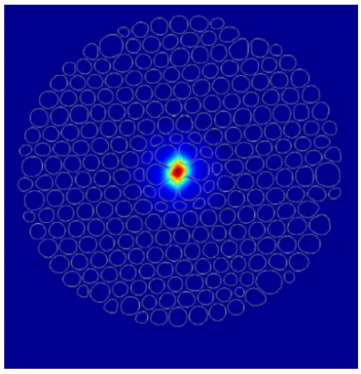

(c) Electric field distribution of the slow-axis mode [28].

Fig. 12 Realistic model simulation.

tion from the waveguide discontinuity region. In the waveguide discontinuity analysis performed in the frequency domain, the electromagnetic field is expressed as

$$\boldsymbol{\Phi} = \boldsymbol{\phi}(x, y, z) \exp(j\omega t) \tag{9}$$

The frequency-domain FEM (FD-FEM) has been widely used for the waveguide discontinuity problems. In the earlier works, FEM was applied to the finite discontinuity region and the mode expansion technique was used for representing infinite uniform waveguides connected to the input and output ports. However, it is difficult and cumbersome to construct the mode expansion boundary condition by taking all the existing modes into account.

Recently, by replacing the input and output ports by anisotropic PML absorbers, the FD-FEM without mode expansion technique has been developed not only for 2D

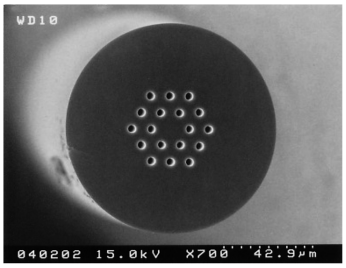

Fig. 13 Single-mode hole-assisted fiber with two air-hole rings [29].

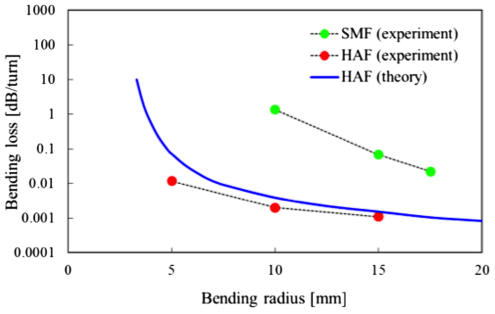

Fig. 14 Bending loss as a function of bending radius at 1550 nm [29].

waveguide discontinuity problems [30] but also for 3D waveguide discontinuity problems [31]. In 2D-FD-FEM, a triangular nodal element shown in Fig. 2(b) is used and in 3D-FD-FEM, on the other hand, a tetrahedral edge element shown in Fig. 5(b) is used.

More recently, using the 2D-FD-FEM, a compact two-mode multi/demultiplexer (TM-MUX) consisting of multimode interference (MMI) waveguides and a wavelength-insensitive phase shifter (PS) was designed for MDM transmission [32]. A silicon-on-insulator (SOI) wafer is assumed and the 3D waveguide structure is replaced by the equivalent 2D waveguide structure with the help of the effective index method. Figure 15(a) shows a schematic drawing of TM-MUX which includes MMI-based mode converter-splitter (MCS), PS with butterfly-shape tapered waveguide structure, and MMI-based 3-dB coupler. Figure 15(b) shows the structure of TM-MUX. Ports 1, 3, and 6 are placed to prevent the reflections at the end of MMI waveguides. Figures 16(a) and (b) show the field distributions of TM-MUX at 1550-nm wavelength for the cases of inputting the fundamental mode and of the first higher-order mode, respectively. When the fundamental mode is input, the fundamental mode is output into port 5. When the first higher-order mode is input, on the other hand, the first higher-order mode is converted into the fundamental mode and is output into port 4. In both cases, little lights are output into the other ports. Therefore, the TM-MUX works as a mode demultiplexer when input port is port 2.

5.2 Time-domain Analysis

Usual BPMs are inadequate for the waveguide discontinuity analysis. Recently, under the condition that the modulation frequency is much lower than the career frequency, a sim-

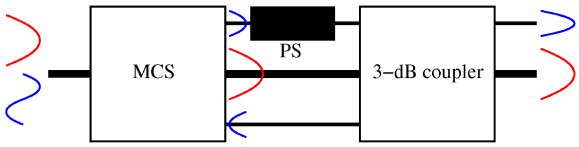

(a) Basic concept of two-mode multi/demultiplexer consisting of a mode converter-splitter, a phase shifter, and a 3-dB coupler.

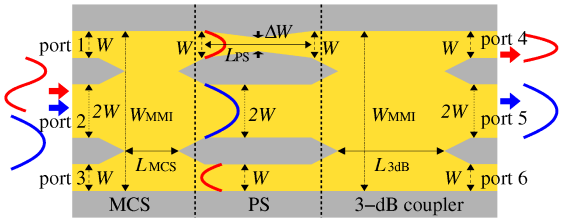

(b) Two-mode multi/demultiplexer constructed with a silicon-on-insulator wafer (top view).

Fig. 15 Compact two-mode multi/demultiplexer [32].

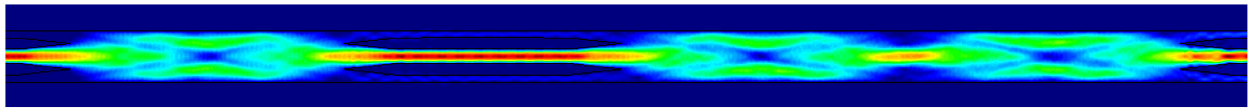

(a) Case of inputting the fundamental mode.

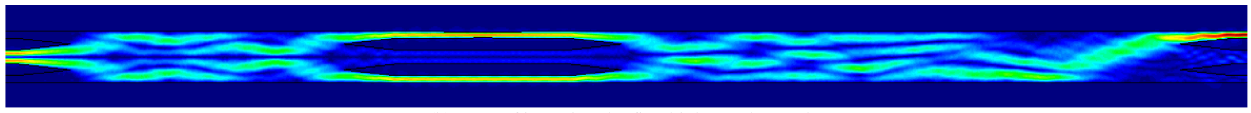

(b) Case of inputting the first higher-order mode.

Fig. 16 Field distributions in two-mode multi/demultiplexer [32].

ple and efficient propagation algorithm was developed and is called the time-domain BPM (TD-BPM). In this algorithm, the electromagnetic field is expressed as

$$\boldsymbol{\Phi} = \boldsymbol{\phi}(x, y, z, t)\exp(j\omega_0 t) \tag{10}$$

where $\boldsymbol{\phi}$ is the modulated envelope and ω_0 is the career center angular frequency.

In the TD-BPM based on FEM (FE-TD-BPM) with anisotropic PMLs [33], the computational spatial domain is discretized with FEM and the Crank-Nicholson algorithm is applied to the time (t) domain. The FE-TD-BPM can tackle waveguide discontinuity problems and a high-performance PML was also developed for PC waveguide discontinuity problems [34]. Recently, a MUX/DEMUX based on PC couplers was proposed and its wavelength demultiplexing properties were investigated by using the FE-TD-BPM [35].

Here, we consider a sharp 90° bend based on PCs composed of dielectric pillars in air on square array with lattice constant of 0.580 μm, where the radius and the refractive index are 0.104 μm and 3.4, respectively [36]. In this structure, almost 100% transmission could be achieved. Figure 17 shows the electric field patterns for the input pulse of career center wavelength of 1.45 μm, where the time step size is taken as 1.0 fs [33]. In the well-known finite-difference time-domain (FDTD) method, very small time step size must be used, compared with FE-TD-BPM, because in FDTD, both the carrier and the modulated envelope are included in the wave propagator. In Fig. 17, the reflected fields from the 90° bend can be hardly observed.

6. Multi-core Fiber Design and Analysis

In current optical fiber transmission systems, transmission capacity is rapidly approaching its fundamental limit. Therefore, an innovative technology is expected to break the limit. In order to overcome this issue, space division multiplexing (SDM) and MDM technologies based on uncoupled MCFs [37], coupled MCFs [38], and few-mode fibers (FMFs) have been investigated actively [39].

The most important issue peculiar to uncoupled MCFs is to reduce the intercore crosstalk. Recently, to estimate the intercore crosstalk in bent and twisted MCFs, a coupled-mode theory (CMT) and a coupled-power theory (CPT) have been newly formulated [40], and an analytical expression for estimating the average intercore crosstalk was also found, resulting in no need for heavy numerical computations [41]. Propagation characteristics of each core and coupling coefficients between two cores in a straight MCF necessary for the solutions of CMT and CPT are accurately evaluated with the full vector FE-ID-BPM which can treat measured refractive-index profiles [42].

Here, we consider a quasi-homogeneous 7-core fiber with nearly identical cores [43] as shown in Fig. 18. Figure 19 shows the bending-diameter dependence of crosstalk from center core 1 to outer cores 2 to 7 calculated with the analytical expression [41], where the dotted line, solid line, dashed line, and dashed and dotted line stand for the correlation lengths of 10 mm, 50 mm, 100 mm, and 500 mm, respectively. The theoretical results with correlation length of 50 mm are in good agreement with the experimental results [43].

In order to realize low crosstalk and a dense core arrangement simultaneously in MCFs, various trench-assisted MCFs (TA-MCFs) such as 7-core fiber with one-pitch layout [44], 10-core fiber with two-pitch layout [45], 12-core fiber with one-ring layout [46], and 12-core fiber with two-ring layout [47] have been developed as shown in Fig. 20. The full vector FE-ID-BPM and the CPT have been effectively utilized for design and analysis of these TA-MCFs.

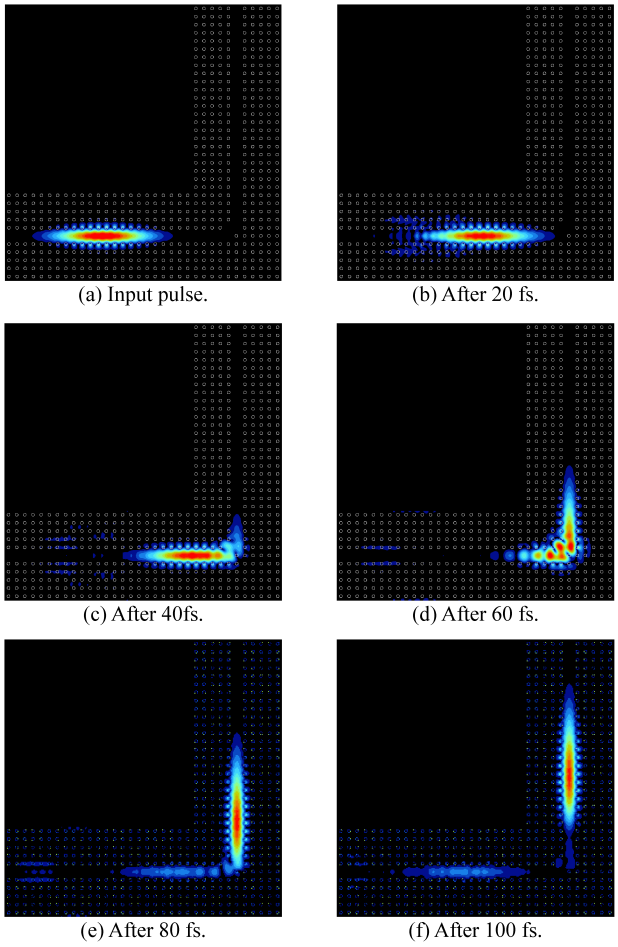

(a) Input pulse. (b) After 20 fs. (c) After 40fs. (d) After 60 fs. (e) After 80 fs. (f) After 100 fs.

Fig. 17 Electric field patterns in photonic crystal bend [33].

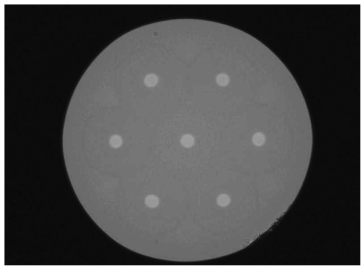

Fig. 18 Quasi-homogeneous multi-core fiber [43].

Most recently, the transmission experiment with the record capacity of 1.01 Pb/s over the one-ring 12-core TA-MCF has been reported [48]

In MDM based on coupled MCFs and FMFs, a mode MUX/DEMUX is needed for exciting and separating different modes [38]. Recently, using the full vector FE-IDBPM for a guided-mode analysis and the full vector FE-BPM for a beam propagation analysis, a fiber-based 1×4 mode MUX/DEMUX was designed for the coupled MCF based MDM [49].

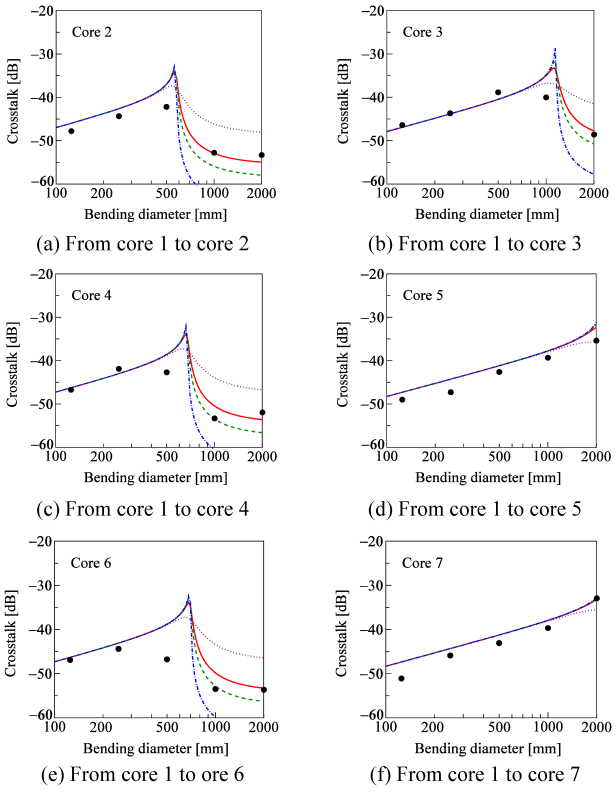

(a) From core 1 to core 2 (b) From core 1 to core 3 (c) From core 1 to core 4 (d) From core 1 to core 5 (e) From core 1 to ore 6 (f) From core 1 to core 7

Fig. 19 Crosstalk from center core 1 to outer cores 2 to 7 [41].

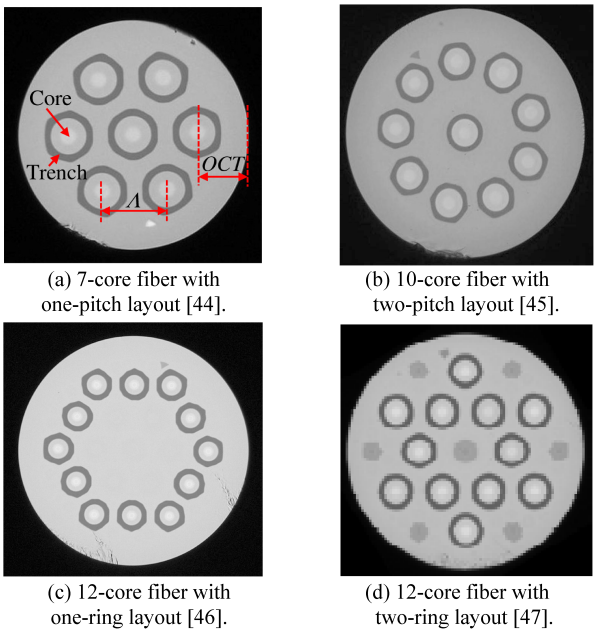

(a) 7-core fiber with one-pitch layout [44]. (b) 10-core fiber with two-pitch layout [45]. (c) 12-core fiber with one-ring layout [46]. (d) 12-core fiber with two-ring layout [47].

Fig. 20 Trench-assisted multi-core fibers.

7. Conclusion

Recent progress in FEM research for optical waveguide design and analysis was reviewed, focusing on the author's works. After briefly reviewing fundamentals of FEM such as a theoretical framework, a conventional nodal element,

a newly developed edge element to eliminate nonphysical, spurious solutions, and a PML to avoid undesirable reflections from computational window edges, various FEM techniques for a guided-mode analysis, a beam propagation analysis, and a waveguide discontinuity analysis were described and some design examples were introduced, including current research activities on MCFs. FEMs have also been applied to design and analysis of various optical waveguide structures with electro-optic effect [50], [51], magneto-optic effect [52],[53], acousto-optic effect [54]–[56], nonlinear effect causing second harmonic generation [57], and instantaneous Kerr-type nonlinear effect [58]–[60].

It is the author's wish that this paper will contribute to the dissemination and development of computational photonics in future.

Acknowledgments

The author would like to express his gratitude to Dr. T. Shibata, Chair of the Editorial Committee for the Special Section on "Recent Advances in Simulation Techniques and Their Applications for Electronics" planned in the IEICE Transactions on Electronics, and to the Committee Members for their encouragement. The author also would like to thank Prof. K. Saitoh of Hokkaido University for helpful discussions. His thanks are also extended to students who worked in his laboratory at Hokkaido University for their Ph.D., M. S., and B. S. theses.

References

[1] J. F. Lee, D. K. Sun, and Z. J. Cendez, "Tangential vector finite elements for electromagnetic field computation," IEEE Trans. Magn. vol. 27, no. 5, pp. 4032–4035, Sept. 1991.
[2] A. F. Peterson, "Vector finite element formulation for scattering from two-dimensional heterogeneous bodies," IEEE Trans. Antennas Propag., vol. 42, no. 3, pp. 357–365, Mar. 1994.
[3] J. P. Berenger, "A perfectly matched layer for the absorption of electromagnetic waves," J. Comput. Phys., vol. 114, no. 2, pp. 185–200, Oct. 1994.
[4] F. L. Teixeira and W. C. Chew, "General closed-form PML constitutive tensors to match arbitrary bianisotropic and dispersive linear media," IEEE Microwave Guided Wave Lett., vol. 8, no. 6, pp. 223–225, June 1998.
[5] M. Koshiba, K. Hayata, and M. Suzuki, "Approximate scalar finite-element analysis of anisotropic optical waveguides," Electron. Lett., vol. 18, no. 10, pp. 411–413, May 1982.
[6] M. Koshiba, K. Hayata, and M. Suzuki, "Approximate scalar finite-element analysis of anisotropic optical waveguides with off-diagonal elements in a permittivity tensor," IEEE Trans. Microw. Theory Tech., vol. MTT-32, no. 6, pp. 587–593, June 1984.
[7] M. Koshiba, K. Hayata, and M. Suzuki, "Vectorial finite-element method without spurious solutions for dielectric waveguide problems," Electron. Lett., vol. 20, no. 10, pp. 409–410, May 1984.
[8] M. Koshiba, K. Hayata, and M. Suzuki, "Improved finite-element formulation in terms of the magnetic field vector for dielectric waveguides," IEEE Trans. Microw. Theory Tech., vol. MTT-33, no. 3, pp. 227–233, Mar. 1985.
[9] M. Koshiba, K. Hayata, and M. Suzuki, "Finite-element solution of anisotropic waveguides with arbitrary tensor permittivity," J. Lightwave Technol., vol. LT-4, no. 2, pp. 121–126, Feb. 1986.
[10] M. Koshiba and K. Inoue, "Simple and efficient finite-element analysis of microwave and optical waveguides," IEEE Trans. Microw. Theory Tech., vol. 40, no. 2, pp. 371–377, Feb. 1992.
[11] M. Koshiba, S. Maruyama, and K. Hirayama, "A vector finite element method with the high-order mixed-interpolation-type triangular elements for optical waveguiding problems," J. Lightwave Technol., vol. 12, no. 3, pp. 495–502, Mar. 1994.
[12] M. Koshiba and Y. Tsuji, "Curvilinear hybrid edge/nodal elements with triangular shape for guided-wave problems," J. Lightwave Technol., vol. 18, no. 5, pp. 737–743, May 2000.
[13] K. Kakihara, N. Kono, K. Saitoh, and M. Koshiba, "Full-vectorial finite element method in a cylindrical coordinate system for loss analysis of photonic wire bends," Opt. Express, vol. 14, no. 23, pp. 11128–11141, Nov. 2006.
[14] T. Murao, K. Saitoh, T. Taru, T. Nagashima, K. Maeda, T. Sasaki, and M. Koshiba, "Bend-insensitive and effectively single-moded all-solid photonic bandgap fibers with heterostructured cladding," European Conference on Optical Communication (ECOC 2009), 2.1.4, Vienna, Austria, Sept. 2009.
[15] Y. Tsuji and M. Koshiba, "Simple and efficient adaptive mesh generation for approximate scalar guided-mode and beam-propagation solutions," IEICE Trans. Electron., vol. E81-C, no. 12, pp. 1814–1820, Dec. 1998.
[16] Y. Tsuji and M. Koshiba, "Adaptive mesh generation for full-vectorial guided-mode and beam-propagation solutions," IEEE J. Selected Top. Quantum Electron., vol. 6, no. 1, pp. 163–169, Jan.-Feb. 2000.
[17] M. Koshiba, Y. Tsuji, and M. Hikari, "Finite element beam propagation method with perfectly matched layer boundary conditions," IEEE Trans. Magn., vol. 35, no. 3, pp. 1482–1485, May 1999.
[18] K. Saitoh and M. Koshiba, "Approximate scalar finite-element beam-propagation method with perfectly matched layers for anisotropic optical waveguides," J. Lightwave Technol., vol. 19, no. 5, pp. 786–792, May 2001.
[19] K. Saitoh and M. Koshiba, "Full-vectorial finite element beam propagation method with perfectly matched layers for anisotropic optical waveguides," J. Lightwave Technol., vol. 19, no. 3, pp. 405–413, Mar. 2001.
[20] Uematsu, K. Saitoh, N. Hanzawa, T. Sakamoto, T. Matsui, K. Tsujikawa, and M. Koshiba, "Low-loss and broadband PLC-type mode (de)multiplexer for mode-division multiplexing transmission," Optical Fiber Communication Conference (OFC 2013), OTh1B.5, Anaheim, USA, Mar. 2013.
[21] Y. Tsuji and M. Koshiba, "Guided-mode and leaky-mode analysis by imaginary distance beam propagation method based on finite element scheme," J. Lightwave Technol., vol. 18, no. 4, pp. 618–623, Apr. 2000.
[22] K. Saitoh and M. Koshiba, "Full-vectorial imaginary-distance beam propagation method based on a finite element scheme: Application to photonic crystal fibers," IEEE J. Quantum Electron., vol. 38, no. 7, pp. 927–933, July 2002.
[23] M. Koshiba, "Full-vector analysis of photonic crystal fibers using the finite element method," IEICE Trans. Electron., vol. E85-C, no. 4, pp. 881–888, Apr. 2002 (invited paper).
[24] K. Saitoh and M. Koshiba, "Numerical modeling of photonic crystal fibers," J. Lightwave Technol., vol. 23, no. 11, pp. 3580–3590, Nov. 2005 (invited paper).
[25] K. Saitoh, T. Murao, L. Rosa, and M. Koshiba, "Effective area limit of large-mode-area solid-core photonic bandgap fibers for fiber laser applications," Opt. Fiber Technol., vol. 16, no. 6, pp. 409–418, Dec. 2010 (invited paper).
[26] M. Koshiba and K. Saitoh, "Finite-element analysis of birefringence and dispersion properties in actual and idealized holey-fiber structures," Appl. Opt., vol. 42, no. 31, pp. 6267–6275, Nov. 2003.
[27] P. J. Roberts, B. J. Mangan, H. Sabert, F. Couny, T. A. Birks, J. C. Knight, and P. St.J. Russell, "Control of dispersion in photonic crystal fibers," J. Opt. Fiber Commun. Rep., vol. 2, no. 5, pp. 435–461,

Nov. 2005.
[28] S. K. Varshney, K. Saitoh, M. Koshiba, and P. J. Roberts, "Analysis of a realistic and idealized dispersion compensating photonic crystal fiber Raman amplifier," Opt. Fiber Technol., vol. 13, no. 2, pp. 174–179, Apr. 2007.
[29] Y. Tsuchida, K. Saitoh, and M. Koshiba, "Design and characterization of single-mode holey fibers with low bending losses," Opt. Express, vol. 13, no. 12, pp. 4770–4779, June 2005.
[30] Y. Tsuji and M. Koshiba, "Finite element method using port truncation by perfectly matched layer boundary conditions for optical waveguide discontinuity problems," J. Lightwave Technol., vol. 20, no. 3, pp. 463–468, Mar. 2002.
[31] Y. Ishizaka, Y. Kawaguchi, K. Saitoh, and M. Koshiba, "Three-dimensional finite-element solutions for crossing slot-waveguides with finite core-height," J. Lightwave Technology, vol. 30, no. 21, pp. 3394–3400, Nov. 2012.
[32] T. Uematsu, Y. Ishizaka, Y. Kawaguchi, K. Saitoh, and M Koshiba, "Design of a compact two-mode multi/demultiplexer consisting of multi-mode interference waveguides and a wavelength insensitive phase shifter for mode-division multiplexing transmission," J. Lightwave Technol., vol. 30, no. 15, pp. 2421–2426, Aug. 2012.
[33] M. Koshiba, Y. Tsuji, and M. Hikari, "Time-domain beam propagation method and its application to photonic crystal circuits," J. Lightwave Technol., vol. 18, no. 1, pp. 102–110, Jan. 2000.
[34] M. Koshiba, Y. Tsuji, and S. Sasaki, "High-performance absorbing boundary conditions for photonic crystal waveguide simulations," IEEE Microwave Wireless Compon. Lett., vol. 11, no. 4, pp. 152–154, Apr. 2001.
[35] M. Koshiba, "Wavelength division multiplexing and demultiplexing with photonic crystal waveguide couplers," J. Lightwave Technol., vol. 19, no. 12, pp. 1970–1975, Dec. 2001.
[36] A. Mekis, J. C. Chen, I. Kurland, S. Fan, P. R. Villeneuve, and J. D. Joannopoulos, "High transmission through sharp bends in photonic crystal waveguides," Phys. Rev. Lett., vol. 77, no. 18, pp. 3787–3790, Oct. 1996.
[37] M. Koshiba, K. Saitoh, and Y. Kokubun, "Heterogeneous multi-core fibers: Proposal and design principle," IEICE Electron. Express, vol. 6, no. 2, pp. 98–103, Jan. 2009.
[38] Y. Kokubun and M. Koshiba, "Novel multi-core fibers for mode division multiplexing: Proposal and design principle," IEICE Electron. Express, vol. 6, no. 8, pp. 522–528, Apr. 2009.
[39] T. Morioka, Y. Awaji, R. Ryf, P. Winzer, D. Richardson, and F. Poletti, "Enhancing optical communications with brand new fibers," IEEE Commun. Magazine, vol. 50, no. 2, pp. S31–S42, Feb. 2012.
[40] M. Koshiba, K. Saitoh, K. Takenaga, and S. Matsuo, "Multi-core fiber design and analysis: Coupled-mode theory and coupled-power theory," Opt. Express, vol. 19, no. 26, pp. B102–B111, Dec. 2011.
[41] M. Koshiba, K. Saitoh, K. Takenaga, and S. Matsuo, "Analytical expression of average power-coupling coefficients for estimating intercore crosstalk in multicore fibers," IEEE Photon. J., vol. 4, no. 5, pp. 1987–1995, Oct. 2012.
[42] K. Saitoh, M. Koshiba, K. Takenaga, and S. Matsuo, "Crosstalk and core density in uncoupled multi-core fibers," IEEE Photon. Technol. Lett., vol. 24, no. 21, pp. 1898–1901, Nov. 2012.
[43] S. Matsuo, K. Takenaga, Y. Arakawa, Y. Sasaki, S. Tanigawa, K. Saitoh, and M. Koshiba, "Crosstalk behavior of cores in multi-core fiber under bent condition," IEICE Electron. Express, vol. 8, no. 6, pp. 385–390, Mar. 2011.
[44] K. Takenaga, Y. Arakawa, Y. Sasaki, S. Tanigawa, S. Matsuo, K. Saitoh, and M. Koshiba, "A large effective area multi-core fiber with an optimized cladding thickness," Opt. Express, vol. 19, no. 26, pp. B543-B550, Dec. 2011.
[45] S. Matsuo, K. Takenaga, Y. Arakawa, Y. Sasaki, S. Tanigawa, K. Saitoh, and M. Koshiba, "Large-effective-area ten-core fiber with cladding diameter of about 200 μm," Opt. Lett., vol. 36, no. 23, pp. 4626–4628, Dec. 2011.
[46] S. Matsuo, Y. Sasaki, T. Akamatsu, I. Ishida, K. Takenaga, K. Okuyama, K. Saitoh, and M. Koshiba, "12-core fiber with one ring structure for extremely large capacity transmission," Opt. Express, vol. 20, no. 27, pp. 28398–28408, Dec. 2012.
[47] A. Sano, H. Takara, T. Kobayashi, H. Kawakami, H. Kishikawa, T. Nakagawa, Y. Miyamoto, Y. Abe, H. Ono, K. Shikama, M. Nagatani, T. Mori, Y. Sasaki, I. Ishida, K. Takenaga, S. Matsuo, K. Saitoh, M. Koshiba, M. Yamada, H. Masuda, and T. Morioka, "409-Tb/s+409-Tb/s crosstalk suppressed bidirectional MCF transmission over 450 km using propagation-direction interleaving," Opt. Express, vol. 21, no. 14, pp. 16777–16783, July 2013.
[48] H. Takara, A. Sano, T. Kobayashi, H. Kubota, H. Kawakami, A. Matsuura, Y. Miyamoto, Y. Abe, H. Ono, K. Shikama, Y. Goto, K. Tsujikawa, Y. Sasaki, I. Ishida, K. Takenaga, S. Matsuo, K. Saitoh, M. Koshiba, and T. Morioka, "1.01-Pb/s (12 SDM/222 WDM/456 Gb/s) crosstalk-managed transmission with 91.4-b/s/Hz aggregate spectral efficiency," European Conference on Optical Communication (ECOC 2012), Th.3.C.1, Amsterdam, The Netherlands, Sept. 2012.
[49] F. Saitoh, K. Saitoh, and M. Koshiba, "A design method of a fiber-based mode multi/demultiplexer for mode-division multiplexing," Opt. Express, vol. 18, no. 5, pp. 4709–4716, Mar. 2010.
[50] M. Koshiba and Y. Tsuji, "Design and modeling of microwave photonic devices," Opt. Quantum Electron., vol. 30, no. 11/12, pp. 995–1003, Dec. 1998 (invited paper).
[51] M. Koshiba, Y. Tsuji, and M. Nishio, "Finite-element modeling of broad-band traveling-wave optical modulators," IEEE Trans. Microw. Theory Tech., vol. 47, no. 9, pp. 1627–1633, Sept. 1999.
[52] M. Koshiba and X.-P. Zhuang, "An efficient finite-element analysis of magnetooptic channel waveguides," J. Lightwave Technol., vol. 11, no. 9, pp. 1453–1458, Sept. 1993.
[53] N. Kono and M. Koshiba, "Three-dimensional finite element analysis of nonreciprocal phase shifts in magneto-photonic crystal waveguides," Opt. Express, vol. 13, no. 23, pp. 9155–9166, Nov. 2005.
[54] K. Saitoh, M. Koshiba, and Y. Tsuji, "Numerical analysis of integrated acoustooptic tunable filters with weighted coupling," J. Lightwave Technol., vol. 17, no. 2, pp. 249–254, Feb. 1999.
[55] K. Saitoh, M. Koshiba, and Y. Tsuji, "Stress analysis method for elastically anisotropic material based optical waveguides and its application to strain-induced optical waveguides," J. Lightwave Technol., vol. 17, no. 2, pp. 255–259, Feb. 1999.
[56] K. Saitoh, M. Koshiba, and Y. Tsuji, "Stress analysis method considering piezoelectric effects and its application to static strain optic devices," J. Lightwave Technol., vol. 17, no. 9, pp. 1626–1633, Sept. 1999.
[57] T. Yasui and M. Koshiba, "Three-dimensional vector beam-propagation method for second harmonic generation analysis," J. Lightwave Technol., vol. 19, no. 5, pp. 780–785, May 2001.
[58] T. Fujisawa and M. Koshiba, "A frequency-domain finite element method for modeling of nonlinear optical waveguide discontinuities," IEEE Photon. Technol. Lett., vol. 16, no. 1, pp. 129–131, Jan. 2004.
[59] T. Fujisawa and M. Koshiba, "Time-domain beam propagation method for nonlinear optical propagation analysis and its application to photonic crystal circuits," J. Lightwave Technol., vol. 22, no. 2, pp. 684–691, Feb. 2004.
[60] T. Fujisawa and M. Koshiba, "Full-vector finite-element beam propagation method for three-dimensional nonlinear optical waveguides," J. Lightwave Technnol., vol. 20, no. 10, pp. 1876–1884, Oct. 2002.

Masanori Koshiba received the B.S., M.S., and Ph.D. degrees in electronic engineering from Hokkaido University, Sapporo, Japan, in 1971, 1973, and 1976, respectively.

In 1976, he joined the Department of Electronic Engineering, Kitami Institute of Technology, Kitami, Japan. From 1979 to 1987, he was an Associate Professor of Electronic Engineering at Hokkaido University, and in 1987, he became a Professor there. From 2013, he serves as a Director of Hokkaido University Career Center. He has been engaged in research on wave electronics, including microwaves, millimeter-waves, lightwaves, surface acoustic waves, magnetostatic waves, and electron waves, and computer-aided design and analysis of guided-wave devices using finite element method, boundary element method, beam propagation method, and so on. He is an author or co-author of more than 400 research papers in refereed international journals. He is an author of books *Optical Waveguide Analysis* (New York: McGraw-Hill, 1992) and *Optical Waveguide Theory by the Finite Element Method* (Tokyo, Japan: KTK Scientific / Dordrecht, The Netherlands: Kluwer Academic, 1992), and is a co-author of the books *Analysis Methods for Electromagnetic Wave Problems* (Boston, MA: Artech House, 1990), *Analysis Methods for Electromagnetic Wave Problems, Vol. Two* (Boston, MA: Artech House, 1996), *Ultrafast and Ultra-parallel Optoelectronics* (Chichester, U.K.: Wiley, 1995), and *Finite Element Software for Microwave Engineering* (New York: Wiley, 1996).

Prof. Koshiba is a fellow of the Institute of Electrical and Electronics Engineers (IEEE) and the Optical Society of America (OSA). In 1987, 1997, and 1999, he was awarded the Excellent Paper Awards from the IEICE, in 1998, the Electronics Award from the IEICE-Electronics Society, in 2004, the Achievement Award from the IEICE, and in 2013, the Distinguished Achievement and Contributions Award from the IEICE. From 1999 to 2000, he served as a President of the IEICE-Electronics Society, and in 2002, he served as a Chair of the IEEE-LEOS (Lasers and Electro-Optics Society, at present, Photonics Society) Japan Chapter. In 2008, he served as a Chair of the IEICE Hokkaido Chapter and from 2009 to 2010, he served as a Vice-President of the IEICE and a Chair of the IEEE Sapporo Section. From 2011 to 2012, he served as a Vice Chair of the IEEE Japan Council.